J Nondestruct Eval (2012) 31:99–107
DOI 10.1007/s10921-011-0125-5

# Evaluation of Equibiaxial Compressive Stress Introduced into Austenitic Stainless Steel Using an Eddy Current Method

**Yuichi Sekine · Hitoshi Soyama**

Received: 28 June 2011 / Accepted: 23 November 2011 / Published online: 1 December 2011


**Abstract** Equibiaxial compressive residual stress is introduced into steel after peening in order to improve both its resistance to stress corrosion cracking and its fatigue strength. Thus, a nondestructive and relatively quick method to evaluate the equibiaxial compressive residual stress in a surface layer modified by peening is required in order to evaluate the peening intensity needed to enhance the integrity of structural components. The purpose of the work reported here is to establish an eddy current method to evaluate equibiaxial compressive stress which can be applied to the residual stress introduced into various non-ferromagnetic materials after peening. To this end, hydraulic jacks were used to elastically deform specimens of the austenitic stainless steel, Japanese Industrial Standard (JIS) SUS316L, thereby introducing an equibiaxial compressive stress. In the case of SUS316L steel, stress-induced martensitic transformation is rare. The electromagnetic properties of these specimens were then measured. In addition, the eddy current signals from peened specimens were compared with these. The results demonstrate that it is possible to establish a method for evaluating the equibiaxial stress utilizing eddy current signals.

**Keywords** Electromagnetic testing · Nondestructive evaluation · Eddy current · Stress · Austenitic stainless steel · Materials testing

Y. Sekine (✉) · H. Soyama
Department of Nanomechanics, Tohoku University, 6-6-01 Aoba, Aramaki, Aoba-ku, Sendai 980-8579, Japan
e-mail: sekine@mm.mech.tohoku.ac.jp

## 1 Introduction

A nondestructive and rapid method to evaluate the equibiaxial compressive residual stress in the surface layer of structural components modified by peening is needed. The introduction of equibiaxial compressive stress by peening is one means of improving the corrosion properties of materials, such as the stress corrosion cracking resistance and the fatigue strength, and therefore, evaluation of this stress is an urgent requirement.

There are various peening methods used to enhance the fatigue strength of metals, such as shot peening (SP) [1], which uses the impact made by shot, cavitation peening (CP) [2], which uses the impact due to cavitation bubbles collapsing, and other peening methods such as laser peening [3]. In previous papers, an improvement in the fatigue strength and the introduction of compressive residual stress after peening have been reported [1–3]. In particular, equibiaxial, rather than uniaxial, compressive residual stress is introduced after peening [4]. The introduction of compressive residual stress improves the corrosion properties such as the stress corrosion cracking resistance. Therefore, a method to evaluate the residual stress is required. If the stress is introduced into paramagnetic materials like austenitic stainless steels, the electrical conductivity varies with stress because of the piezoresistive effect [5]. Measuring stress using variations in the electromagnetic properties is an effective, nondestructive, relatively quick method for inspecting metallic structures.

There are a number of methods that use electromagnetic properties to evaluate the residual stress in the surface layers of metallic components, such as the potential drop technique [6], the Barkhausen method [7], and the eddy current method [5, 8, 9]. In the present paper, we examine the eddy current method in order to establish a rapid nondestructive

test for measuring stress in the surface layers of various metallic materials, including paramagnetic and ferromagnetic materials. Using this method, the authors previously showed that the electromagnetic properties of the surface of alloy tool steel, Japanese Industrial Standard (JIS) SKD61, peened by CP varied with processing time [10]. Also using this method, the electrical conductivity in shot-peened nickel-base superalloys was found to vary [8, 9]. Blodgett and Nagy used an eddy current method to show that the electrical conductivity varied with axial stress [5]. Blaszkiewicz investigated the relationship between the signal from the eddy current and the residual stress introduced by flexing the specimen in a vise [11]. However, the relationship between equibiaxial stress induced by peening and by elastic deformation is unknown, because concomitant plastic deformation can increase or decrease dislocations causing changes to the electromagnetic properties [12]. Thus, to establish a method to evaluate stress in metallic materials using variations in the electromagnetic properties, a method that can evaluate stress that does not disturb the microstructure, is required.

In the present paper, in order to avoid microstructural changes such as the introduction of dislocations, hydraulic jacks were used to induce equibiaxial compressive stress into SUS316L specimens, and the electromagnetic properties were measured using the eddy current method. Using hydraulic jacks introduces elastic deformation without plastic deformation. The results show that electromagnetic parameters such as the electrical conductivity vary with the applied compressive stress. To compare stress introduced by hydraulic jacks with the stress introduced by peening, specimens peened by CP which scarcely causes plastic deformation compared to SP were also evaluated using the eddy current method. Note that this is the first report to show a variation of the electromagnetic properties with the introduced equibiaxial stress using an eddy current method.

## 2 Experimental Apparatus and Method

The test material was JIS SUS316L austenitic stainless steel. The chemical composition of all specimens made of JIS SUS316L correspond to AISI 316L type stainless steel [13, pp. 3–13]. General thermal refining of the JIS SUS316L steel was conducted. The chemical composition of the stainless steel used in the study is as follows: 0.014% C, 0.6% Si, 1.0% Mn, 0.03% P, 0.004% S, 12.0% Ni, 17.5% Cr, 2.1% Mo and the balance is made up with Fe. The 0.2% yield strength was 304 MPa, and the tensile strength was 576 MPa. The grain size was $20 \pm 7$ μm. The length, width and height of the specimen to which equibiaxial stress was applied were 16, 16, 10 mm, respectively, and this was designated the equibiaxial specimen. Figure 1 shows

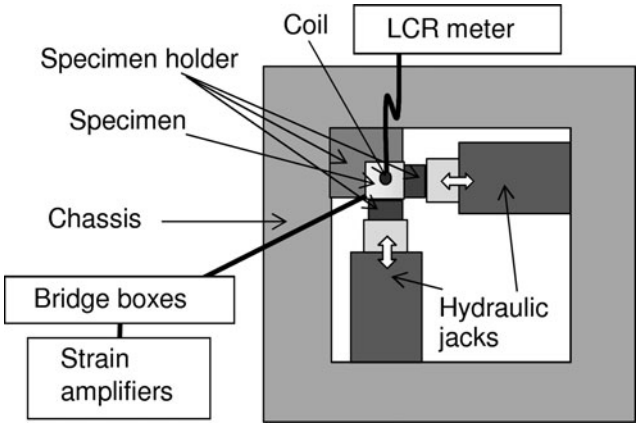


**Fig. 1** Schematic illustration of the experimental apparatus used for introducing equibiaxial compressive stress

a schematic illustration of the experimental setup for introducing equibiaxial stress. The equibiaxial stress, $\sigma_b$, is introduced by two hydraulic jacks as shown in Fig. 1. Strain gauges are attached to the underside of the specimen, and on the upper side is a coil for eddy current testing. The electromagnetic properties evaluated by the eddy current method were compared with the stress measured by the strain gauges. Young's modulus and Poisson's ratio of the material under test were assumed to be 193 GPa and 0.3, respectively. In the present study, the induced stress was considered to be plane stress condition. The specimen holders illustrated in Fig. 1 were made of SUS316L.

For comparison, the residual stresses induced in specimens peened by CP, designated as CP specimens, were also evaluated by the eddy current method. The size of the CP specimens was determined by considering the edge effect of the eddy current. The thickness, width and length of the specimen were 6, 100 and 200 mm, respectively. CP was conducted at the center of the specimen. Therefore, in the present study, two types of specimen, equibiaxial and CP specimens, were used. The CP conditions were determined based on previous results and conditions [14]. A high-speed water jet pressurized to 30 MPa by a plunger pump was injected into a low-speed water jet and discharged into air. The pressure of the low-speed water jet was 0.05 MPa. The nozzle diameter was 1 mm and the distance between the nozzle and the specimen, the standoff distance, was 45 mm. The processing time per unit length, $t_p$, was determined as follows,

$$t_p = \frac{n}{v} \tag{1}$$

$n$ denotes the number of scans, and $v$ denotes the scanning speed. In the present study, $t_p$ was varied to introduce different residual stresses into each specimen. The CP specimens are used to determine how the electromagnetic properties vary with residual stress introduced by CP and to compare this with the equibiaxial stress introduced by the hydraulic

**Table 1** Properties of the coil

| Properties | | Values |
|---|---|---|
| Number of turns | $N$ (turns) | 240 |
| Wire diameter | $d_w$ (mm) | 0.1 |
| Outer diameter | $2r_2$ (mm) | 6.9 |
| Inner diameter | $2r_1$ (mm) | 3.0 |
| Lift off | $s$ (mm) | 0.3 |
| Thickness | $h_{\text{coil}}$ (mm) | 2 |

jacks. To vary the compressive residual stress, 7 CP specimens with $t_p = 0.25, 0.5, 1, 2, 5, 10$ and 20 s/mm and a non-peened (NP) control specimen were prepared. The CP scanning direction was normal to the longitudinal direction. The roughness of the NP specimen was $0.12 \pm 0.01$ μm, and that of the CP specimen at $t_p = 20$ s/mm was $0.86 \pm 0.10$ μm. Erosion due to peening did not occur in the samples in the present study. Also, the samples were not polished during the experiments.

The eddy current testing was conducted by measuring the coil reactance, $X$, as a function of the frequency, $f$, of the coil to investigate changes in the electromagnetic properties such as the electrical conductivity. $X$ as a function of $f$ was measured 3 times at the center of the specimen using an LCR meter, HIOKI 3532-50, connected directly to the coil, and the average value only of $X$ was calculated, considering the variation of the coil resistance with $f$ due to the phase rotation derived from the instrumentation effect, the sensitivity of the coil lift off variation and stress. The resolution in the LCR meter measurements of $X$ for $1 \le X < 10\ \Omega$, $10 \le X < 100\ \Omega$, $100 \le X < 1000\ \Omega$, and $1000 \le X < 10000\ \Omega$ were 0.0001, 0.001, 0.01, 0.1 Ω, respectively. In the present study, to reduce the effect of thermal drift, the tests were conducted at room temperature, and the eddy current test was conducted more than 60 minutes after the power of the LCR meter was switched on. Table 1 shows the coil parameters used in this study. The ratio of the inductance at $f = 400$ kHz compared with that at $f = 1$ kHz was 1.02. In the present study, no compensation was applied to $X$ for the inductance ratio and no assumptions were made regarding the equivalent circuit of the coil. The amplitude of the current driven by the LCR meter was 0.8 mA. With this and with $f = 400$ kHz, the measurement accuracy of $X$ was 0.8%.

The penetration depth, $\delta$, when using an alternating current with frequency $f$ is given by (2) [15]

$$\delta = \frac{1}{\sqrt{\pi f \mu (\frac{1}{\rho})}} \tag{2}$$

where $\mu$ denotes the permeability and $\rho$ denotes the electrical resistivity. In the present study, the resistivity and relative permeability used for calculating the penetration depth of the eddy current are assumed to be $74 \times 10^{-8}$ Ωm and 1.003, respectively [13, pp. 489–494]. With $f = 400$ kHz, $\delta$ is calculated to be 0.7 mm from (2).

Stress-induced martensitic transformation hardly occurs in the case of SUS316L steel. If it does occur after processing, the ferrite phase and the magnetic permeability increase. From the residual austenitic ratio calculated from the integrated intensities of the X-ray diffraction profiles of both the $\alpha$-Fe phase and the $\gamma$-Fe phase, the residual austenitic volume ratio of 3 NP specimens was found to be $91 \pm 4\%$, and that of a CP specimen at $t_p = 20$ s/mm was 91.2%. Thus, it was concluded that the deformation-induced martensitic transformation did not occur after CP. Thus, in this study, only the variation in $\rho$, the inverse of the conductivity, and not the magnetic permeability was considered after the introduction of the compressive equibiaxial stress. The method, however, cannot be applied to SUS 304, for example, because of the martensitic transformation.

The impedance of the coil above the specimen was calculated using the Cheng-Dodd-Deeds model [16]. The coil geometry, parameters and models for the calculation are shown in Fig. 2. Figure 2(a) is the model used for the equibiaxial specimen and Fig. 2(b) is that used for the CP specimen. In Fig. 2, $z_1, z_2$ denote the $z$-coordinates of the bottom and top, respectively ($z_1, z_2 > 0$). $d_k$ denotes the distance between the surface and the bottom of the $k$th layer as shown in Fig. 2. In Fig. 2(b), $d_k$ ($1 \le k \le 6$) were determined from the thickness of the surface modified layer, $\zeta$, derived from Ref. [14]. $\zeta$ varies with $t_p$ as shown by the results of Ref. [14]. The relationship between $\zeta$ (mm) and $t_p$ (s/mm) is given by the following [14]:

$$\zeta = 0.270\left(1 - e^{-4.87 t_p}\right) + 0.149\left(1 - e^{-\frac{4.87}{21.5} t_p}\right) \tag{3}$$

The peened layer is divided into 6 layers of equal thickness. The electromagnetic properties of layers larger than $z = \zeta = d_6$ were set to the following reference values: relative permeability, $\mu_r = 1.003$, and $\rho = 74 \times 10^{-8}$ Ωm [13, pp. 489–494]. In calculating $\rho$ for the CP specimen, we take into account that the electrical resistivity of the $k$th layer, $\rho_k$, has a linear relationship with $z$ because the residual stress, $\sigma_R$, has a linear relationship with $z$ in the case of SUS316L after CP treatment [14].

The impedance of the coil in free space, $Z_0$, can be written as follows:

$$Z_0 = j\omega K \int_0^\infty \frac{Int^2(qr_1, qr_2)}{q^5} \times \left\{(z_2 - z_1) + \frac{\exp[-q(z_2 - z_1)] - 1}{q}\right\} dq \tag{4}$$

where

$$K = \frac{2\pi \mu_0 N^2}{(r_2 - r_1)^2 (z_2 - z_1)^2} \tag{5}$$

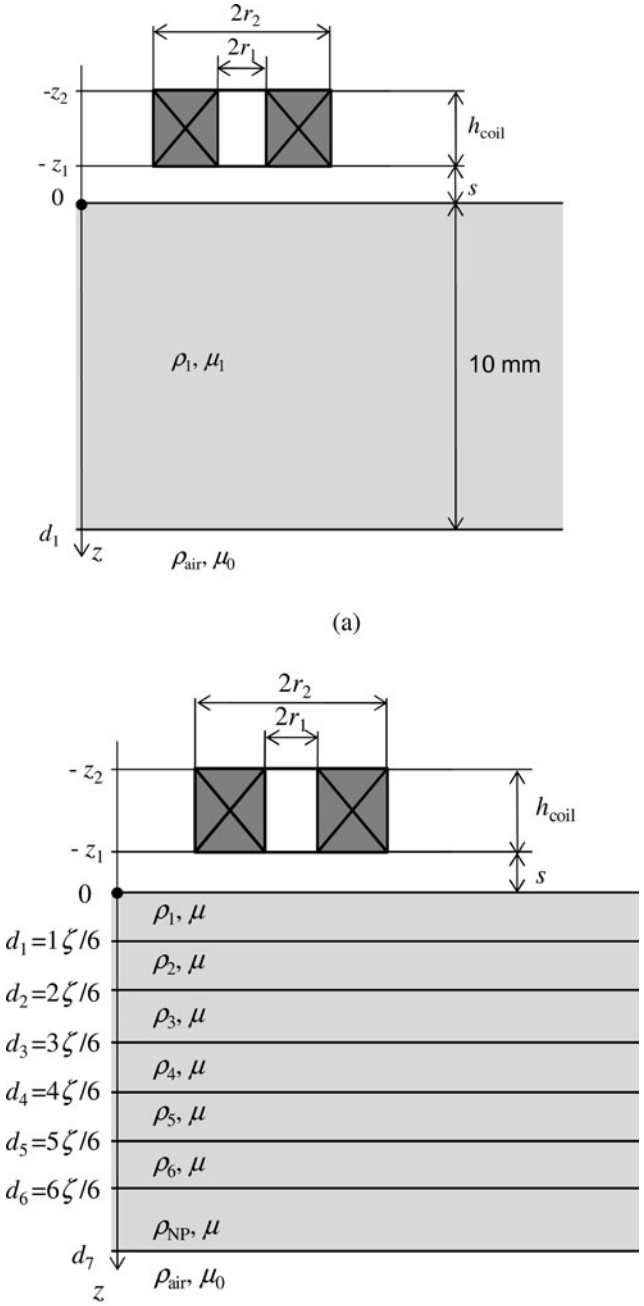


**Fig. 2** Cross-section of the coil and models used for calculations using the Cheng-Dodd-Deeds model. (**a**) Model used for the equibiaxial specimen. (**b**) Model used for the CP specimen

$$Int^2(s_1, s_2) = \int_{s_1}^{s_2} s J_1(s) ds \tag{6}$$

$J_1(x)$ denotes the Bessel function of the first kind and first order.

The impedance change, $\Delta Z$, of the coil placed on the multilayer specimen is given by

$$\begin{aligned}\Delta Z &= j\omega K \int_0^\infty \frac{Int^2(qr_1, qr_2)[\exp(-qz_1) - \exp(-qz_2)]^2}{q^6} \\ &\quad \times \frac{q\mu_r - p}{q\mu_r + p} dq \\ &= j\omega K \int_0^\infty \frac{Int^2(qr_1, qr_2)[\exp(-qz_1) - \exp(-qz_2)]^2}{q^6} \\ &\quad \times \frac{V_1}{U_1} dq \end{aligned} \tag{7}$$

where

$$p = \sqrt{q^2 + j\omega\mu_r\mu_0\left(\frac{1}{\rho}\right)} \tag{8}$$

$\omega$, $\mu_r$ and $\mu_0$ denote the angular frequency, relative magnetic permeability and the permeability of air, which is $4\pi \times 10^{-7}$ H/m, respectively. In the present paper, $\mu_r$ is set as the reference value for 316 type stainless steel, where $\mu_r = 1.003$ [13, pp. 489–494]. The term, $V_1/U_1$, in (7) represents the conductor reflection coefficient. These equations apply to an infinite solution region, which presents us with some numerical difficulties. Applying the extended truncated region eigenfunction expansion (ETREE) method [17, 18] which, based on the analytical method of Theodoulidis and Kriezis [19], assumes that the solution region is finite in the radial direction, (4) and (7) can be rewritten as follows [19]:

$$\begin{aligned} Z_0 &= j\omega K \sum_{i=1}^{\infty} \frac{Int^2(q_i r_1, q_i r_2)}{[(q_i b) J_0(q_i b)]^2 q_i^5} \\ &\quad \times 2\{q_i(z_2 - z_1) - 1 + \exp[-q_i(z_2 - z_1)]\} \end{aligned} \tag{9}$$

$$\begin{aligned} \Delta Z &= j\omega K \\ &\quad \times \sum_{i=1}^{\infty} \frac{Int^2(q_i r_1, q_i r_2)[\exp(-q_i z_1) - \exp(-q_i z_2)]^2}{[(q_i b) J_0(q_i b)]^2 q_i^5} \\ &\quad \times \frac{V_1}{U_1} \end{aligned} \tag{10}$$

where [18]

$$J_1(q_i b) = 0 \tag{11}$$

$$\begin{cases} U_k = \left(\dfrac{p_{k-1}}{\mu_{k-1}} - \dfrac{p_k}{\mu_k}\right) e^{-2p_k(d_k - d_{k-1})} V_{k+1} \\ \qquad + \left(\dfrac{p_{k-1}}{\mu_{k-1}} + \dfrac{p_k}{\mu_k}\right) U_{k+1} \\ V_k = \left(\dfrac{p_{k-1}}{\mu_{k-1}} + \dfrac{p_k}{\mu_k}\right) e^{-2p_k(d_k - d_{k-1})} V_{k+1} \\ \qquad + \left(\dfrac{p_{k-1}}{\mu_{k-1}} - \dfrac{p_k}{\mu_k}\right) U_{k+1} \end{cases} \tag{12}$$

$$U_M = \frac{p_{M-1}}{\mu_{M-1}} + \frac{p_M}{\mu_M} \tag{13}$$

$$V_M = \frac{p_{M-1}}{\mu_{M-1}} - \frac{p_M}{\mu_M} \tag{14}$$

$$p_M = \sqrt{q_i^2 + j\omega\mu_0\mu_M\left(\frac{1}{\rho_M}\right)} \tag{15}$$

$$p_0 = q_i \tag{16}$$

$J_1$ is a Bessel function of the first kind of order 1. $b$ denotes the solution region which was set to a size such that it had no effect on the calculation. $p_i$ denotes the discrete eigenvalue. $U_k$ and $V_k$ indicate that the formulae are recursive. $k = M$ signifies a semi-infinite free-space layer, and the electromagnetic properties of the layer are as follows, $\rho_M = +\infty$ Ωm and $\mu_M = 1$. $M$ was set to 2 for the equibiaxial specimen as shown in Fig. 2(a), and set to 8 for the CP specimens as shown in Fig. 2(b). To analyze the resistivity from the eddy current results of the CP specimens, the values of $\rho_k$ of the top 6 layers in Fig. 2(b) were set such as to minimize the error between the calculated and measured reactance, taking account of the stress profile as a function of depth from Ref. [14] and assuming that the relationship between the stress and resistivity is linear, i.e. the piezoresistive coefficient is constant. Considering the intensity of the eddy current with depth, the resistivity at the smaller $z$ in each layer in Fig. 2(b) was used to determine the standard resistivity. From measurements of the full widths at half maximum (FWHM) of the X-ray diffraction profiles, the plastic deformation caused by CP is at a relatively lower level than that from SP, and so its effect on the eddy current results is less and limited to a depth less than $d_2$ in Fig. 2(b). In the present study, the effect of plastic deformation on the eddy current results was not considered.

To compare the stress induced by the hydraulic jacks and that introduced by CP, the actual stress at the surface is required. The stresses in the CP specimens and the equibiaxial specimen without loading were measured using an X-ray diffraction $\sin^2\psi$ method. A Cr tube, operating at 30 kV and 8 mA, was used to produce K$\beta$ X-rays. The angles between the normal to the surface and the normal to the lattice plane, $\psi$, were 0, 22.8, 33.2, 42.1 and 50.7 deg. X-rays were counted for 4 s for each step using a scintillation counter. The diffractive plane was the (311) plane of $\gamma$-Fe, and the diffractive angle without strain, $2\theta_0$, was 148.5 deg. Diffractive angle measurements from 143 to 153 deg in 0.2 deg steps were made. Under the present conditions, the stress factor was −369.5 MPa/deg.

## 3 Results

Figure 3 shows the reactance, $X$, of the coil in air, $X_{\text{air}}$, and the reactances with the specimen with $\sigma_b = 0$ MPa, $X_{0\,\text{MPa}}$, and with $\sigma_b = -200$ MPa, $X_{-200\,\text{MPa}}$, as functions of frequency, $f$. $X$ is the imaginary part of the coil impedance, $Z$. These were used as standard values in calculating impedance using the Cheng-Dodd-Deeds model.

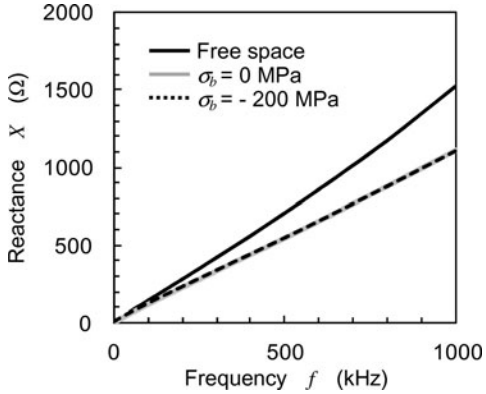


**Fig. 3** Variation of reactance with frequency

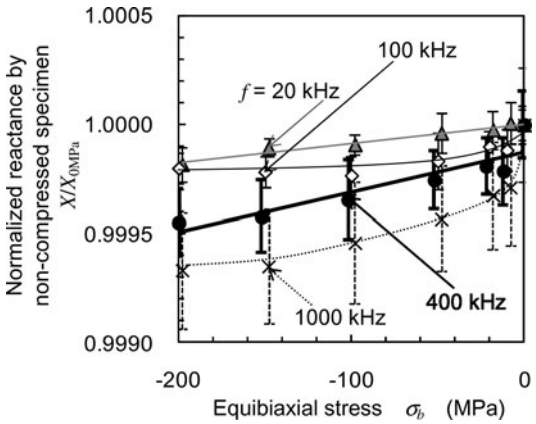


**Fig. 4** Variation of coil reactance normalized by $\sigma_b = 0$ MPa with the equibiaxial compressive stress at various frequencies

From Fig. 3, $X_{\text{air}}$ increases proportionally with $f$, and this tendency is consistent with the theory.

Figure 4 shows the variation with $\sigma_b$ of the reactance, $X$, normalized to the non-compressed specimen at $f = 20, 100, 400, 1000$ kHz. From Fig. 4, the variation of $X/X_{0\,\text{MPa}}$ increases with $f$. In general, the quantity of eddy current generated in metallic materials increases with $f$. Thus, the variation of $X/X_{0\,\text{MPa}}$ increases with $f$. However, the relationship between $X/X_{0\,\text{MPa}}$ and $\sigma_b$ is nonlinear with $f = 100$ and 1000 kHz because of the measurement resolution limits. Thus, an appropriate $f$ at which the equibiaxial stress should be evaluated needs to be selected. The large error bars may be derived from the measurement accuracy of the LCR meter and the up and down movement of the coil. Incidentally, from 10 measurements of $X$ of the NP specimen with the affect of the up and down movement of the coil, the normalized standard deviation of the average value of $X$ at $f = 400$ kHz was 0.0003. In addition, thermal drifting at $f = 400$ kHz causes a variation of 0.00007 of the normalized reactance which is smaller than the variation due to the introduction of equibiaxial compressive stress. In addition, it was shown that movement of the coil and the dis-

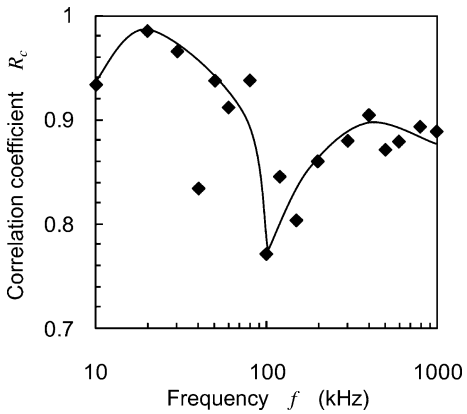


**Fig. 5** Variation of correlation coefficient between normalized reactance and equibiaxial stress with frequency

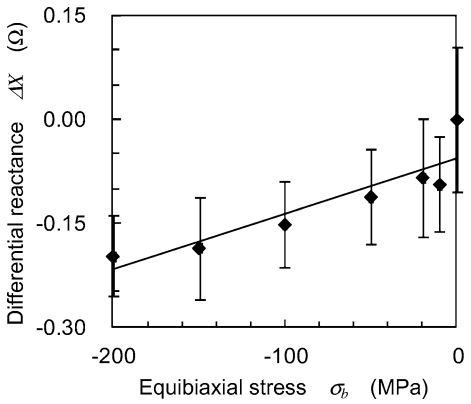


**Fig. 6** Variation of differential reactance with the equibiaxial compressive stress at $f = 400$ kHz

tance between the coil and the specimen holder, as shown in Fig. 1, had little effect on the eddy current results.

To choose an appropriate $f$, we examined the correlation coefficient, $R_c$, between $X/X_{0\,\mathrm{MPa}}$ and $\sigma_b$ as a function of frequency, and this is shown in Fig. 5. If there are $n$ pairs of coordinates $(x_i, y_i)$, the average of these, $(\overline{x}, \overline{y})$, $R_c$ is defined as follows:

$$R_c = \frac{\sum_{i=1}^{n}(x_i - \overline{x})(y_i - \overline{y})}{\sqrt{\sum_{i=1}^{n}(x_i - \overline{x})^2}\sqrt{\sum_{i=1}^{n}(y_i - \overline{y})^2}} \tag{17}$$

The definition of $R_c$ is based on statistical science, and from the definition it has no units of measurement. $R_c$ shows the correlation between $x$ and $y$. If $R_c$ is close to $\pm 1$, the $n$ plots consisting of $(x_i, y_i)$ are arranged on a line. If $R_c$ is close to 0, the $n$ plots consisting of $(x_i, y_i)$ are not arranged on a line, and it can be concluded that there is no correlation between them. To calculate $R_c$ for the linear relationship between $\sigma_b$ and $X/X_{0\,\mathrm{MPa}}$, they are substituted for $x$ and $y$ in (17). From Fig. 5, we see that $R_c$ is high at relatively low $f$. The induced eddy current increases with $f$. At higher $f$, noise and the surrounding conditions affect the result more than at lower $f$. However, the eddy current is small at low $f$. To evaluate the equibiaxial stress, the accuracy of the measurement is greater at higher $f$ because the variation of $X$ by the introduction of equibiaxial compressive stress increases with $f$. In addition, the cause of low $R_c$ at $f = 100$ kHz, as shown in Fig. 5 is the limiting measurement resolution. The values of $X_{0\,\mathrm{MPa}}$ at $f = 80$ and 100 kHz are 97.83 Ω and 120.4 Ω, respectively. From these, the resolution capability of $X$ at $f = 100$ kHz is worse than that at $f = 80$ kHz. The differences between $X_{-200\,\mathrm{MPa}}$ and $X_{0\,\mathrm{MPa}}$ at $f = 80$ and 100 kHz were 0.019 and 0.02 Ω, respectively, considering the resolution capability. In the case of $f = 100$ kHz, it was difficult to detect the variation in stress because there is only one significant digit. With induced stress, the difference between $X_{-200\,\mathrm{MPa}}$ and $X_{0\,\mathrm{MPa}}$ increases with $f$, shown by the raw data for $X$ given in Fig. 3. Thus, a dip in $R_c$ appears at $f = 100$ kHz. Besides, $\delta$ at $f = 400$ kHz is calculated to be 0.7 mm, and $\delta$ at $f = 20$ kHz is 3 mm from (2). Taking these values of $\delta$ into account, in evaluating the peened layer, a higher value of $f$ is more appropriate for measurements employing the eddy current method. In the present study, taking account of $R_c$ in Fig. 5, the variation in reactance in Fig. 4 and $\delta$ calculated from (2) applied to the evaluation of the peened layer, $X$ at $f = 400$ kHz was chosen to evaluate the equibiaxial stress.

Figure 6 shows the variation in differential reactance, $\Delta X$, at $f = 400$ kHz with $\sigma_b$. $\Delta X$ is the difference between $X$ and $X_{0\,\mathrm{MPa}}$. From Fig. 6, $X$ decreases with equibiaxial compressive stress. The cause of the decrease in $X$ is a decrease in electrical resistivity, $\rho$. The equibiaxial compressive stress was introduced into the specimen by elastic deformation using the hydraulic jacks, and variations in the microstructure, such as an increase in dislocations, did not occur. Thus, the decrease in $\rho$ is derived from the piezoresistive effect [5].

To establish the relationship between the piezoresistive effect and the equibiaxial compressive stress, the variation of $\rho$ with equibiaxial compressive stress was investigated using numerical analysis. Figure 7 shows the electrical resistivity, $\rho_1$, calculated using the model shown in Fig. 2(a), varying with equibiaxial compressive stress, calculated using (9) and (10). The resistivity at $\sigma_b = 0$ MPa, $\rho_{0\,\mathrm{MPa}}$, is taken as a reference value, where $\rho_{0\,\mathrm{MPa}} = 74 \times 10^{-8}$ Ωm [13, pp. 489–494], and $\rho_1$ is normalized to $\rho_{0\,\mathrm{MPa}}$ in Fig. 7. From Fig. 7, $\rho_1$ decreases with the equibiaxial compressive stress because of the piezoresistive effect. The gradient of $\rho_1/\rho_{0\,\mathrm{MPa}}$ with respect to $\sigma_b$ is $30 \pm 20$ TPa$^{-1}$. The chemical composition of JIS SUS316L shows iron to be the major component of SUS316L. Comparing this with the reference value of Fe, which is 24 TPa$^{-1}$ calculated from the relationship between the resistivity and induced stress [20], the equibiaxial compressive stress can be evaluated from the variation of the electrical resistivity.

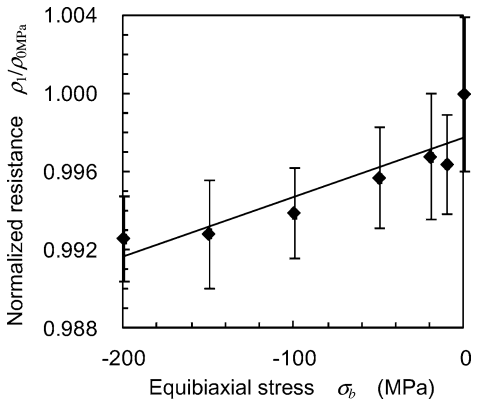


**Fig. 7** Variation of electrical resistivity with the equibiaxial compressive stress calculated using the Cheng-Dodd-Deeds model at $f = 400$ kHz

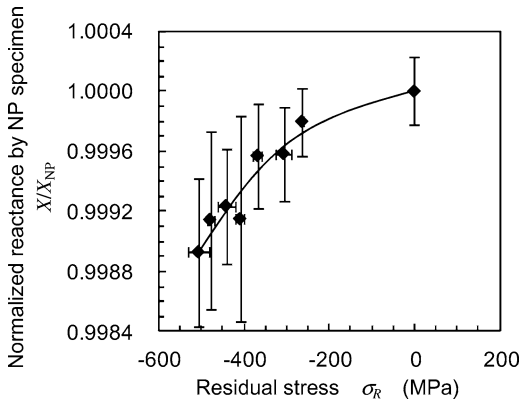


**Fig. 8** Variation of the normalized reactance of the CP specimen with residual stress at the surface at $f = 400$ kHz

To establish this as a method for evaluating the equibiaxial compressive stress in peened materials, we compared the results for the equibiaxial specimen with those for a CP specimen, in which the microstructural changes are relatively small. Figure 8 shows the relationship between coil reactance and stress at the surface of the CP specimen. The large error bars in Fig. 8 may be derived from the measurement accuracy of the LCR meter and the affect of the up and down movement of the coil. In addition, from the peened and annealed specimens, which was used to relieve the residual stress while maintaining the surface roughness, it was shown that the surface roughness had little affect on the eddy current result. In both Figs. 6 and 8, $X$ decreases with induced compressive stress. In Fig. 8, the variation of $X$ increases with the introduced compressive residual stress. The variation of $X$ is affected by the penetration depth, $\delta$, calculated from (2) and the thickness of the modified layer where the compressive residual stress is introduced by CP. The stress distributions of the equibiaxial and peened specimens are different. The variation in resistivity due to the introduction of stress causes variations in $X$. Thus, $X$ alone

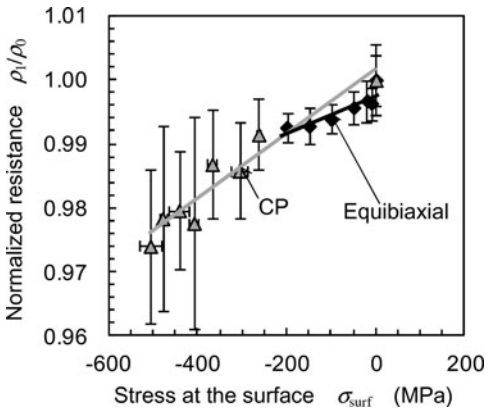


**Fig. 9** Variation of electrical resistivity with stress at the surface at $f = 400$ kHz

cannot be used to evaluate the equibiaxial stress induced by peening. To estimate the equibiaxial stress induced by peening, the distribution in resistivity has to be assumed from the stress distribution. Moreover, the variation of the electromagnetic parameters with equibiaxial stress induced by hydraulic jacks and peening should be established. Thus, the equibiaxial compressive stress induced by peening techniques cannot be evaluated from the variation of $X$ obtained by eddy current testing. Instead of using $X$, the equibiaxial compressive stress for the peened materials should be evaluated using the variation in $\rho$, taking account of the thickness of the modified layer and the depth distribution of the residual stress. In the case of CP, $\sigma_R$ has a linear relationship with $z$ [14]. Thus, for calculating $\rho$, the model shown in Fig. 2(b) was used for the CP specimen and it was assumed that $\rho_k$ had a linear relationship with $z$ based on constant piezoresistivity.

To establish the method for evaluating equibiaxial stress, $\rho$ was compared to the stress at the surface, $\sigma_{surf}$. To apply the stress measurement using the eddy current method for peened materials, the variation in $\rho$ with equibiaxial compressive stress should be compared with the variation in $\rho$ with the stress induced by peening. The electrical resistivity of the top layer, $\rho_1$, shown in Fig. 2, was used. Figure 9 shows a comparison of the relationships between $\rho_1$ and $\sigma_{surf}$ for both the equibiaxial and CP specimens. Note that, $\rho_1$ of the equibiaxial specimen was obtained from the model shown in Fig. 2(a), and $\rho_1$ of the CP specimen was obtained from that in Fig. 2(b). The resistivity is normalized by that of the control specimen, $\rho_0$, assumed to be $\rho_0 = 74 \times 10^{-8}$ Ωm. This value is the non-peened (NP) specimen for the CP specimen and the non-compressed specimen for the equibiaxial specimen. In addition, considering the yield strength, the minimum equibiaxial stress was set as $\sigma_b = -200$ MPa. From Fig. 9, $\rho_1$ of both the equibiaxial and CP specimens decreases with compressive stress because of the piezoresistive effect, and the relationship between $\rho_1/\rho_0$ and $\sigma_{surf}$ in both cases is linear. The gradient

between $\rho_1/\rho_0$ and $\sigma_b$ of the CP specimen shown in Fig. 9 is $50 \pm 30$ TPa$^{-1}$. The reference value is 24 TPa$^{-1}$, which is the value for Fe, considering it is the major component [20], and the gradient of the equibiaxial specimen obtained from Fig. 7 is $30 \pm 20$ TPa$^{-1}$. Considering the confidence limit, the variation in resistivity of the CP specimen is related to the introduction of equibiaxial compressive stress. From the results, a method to evaluate equibiaxial stress induced by peening using eddy current signals can be established. The large piezoresistive coefficient and error bars of the CP specimens seem to be derived from the measurement accuracy obtained with a moving coil, the difference between the chemical composition of SUS316L and pure iron, and the assumptions about the depth distribution of the resistivity. Moreover, when the thickness of the peened layer is needed to determine the peening intensity, an additional inverse analysis using variation of the electromagnetic properties after peening should be done.

## 4 Conclusions

In order to establish a method for evaluating the residual stress in a surface layer modified by peening, the equibiaxial compressive stress, induced into a specimen of SUS316L by elastic deformation using hydraulic jacks, was measured by evaluating the electromagnetic properties of the specimen using an eddy current method. The electromagnetic properties of a specimen peened by cavitation peening (CP) were also measured by the eddy current method in order to compare it with the mechanically loaded specimen. The reactance measured in the eddy current test was used to evaluate the equibiaxial stress. The results obtained are summarized below:

(1) The reactance at 400 kHz decreases with the elastically induced equibiaxial compressive stress. It is possible to evaluate the equibiaxial compressive stress by measuring the reactance of the coil used in the eddy current measurements.
(2) The electrical resistivity decreases with the elastically induced equibiaxial compressive stress. The variation in electrical resistivity can be used to evaluate the equibiaxial compressive stress.
(3) The reactance at 400 kHz and electrical resistivity of the CP specimen decrease with induced stress. The variation in resistivity of the CP specimen is related to the introduction of equibiaxial compressive stress. Thus, it is possible to establish a method to evaluate the equibiaxial stress induced by peening using eddy current signals.

**Acknowledgements** This work was partly supported by the Japan Society for the Promotion of Science under a Grant-in-Aid for Scientific Research 21 · 3334.

**Table 2** FWHM of CP specimens

| $t_p$ (s/mm) | FWHM (deg) | $\zeta_F$ (mm) |
|---|---|---|
| 0 (NP) | 1.457 | – |
| 0.25 | 1.477 | 0.004 |
| 0.5 | 1.481 | 0.008 |
| 1 | 1.500 | 0.008 |
| 2 | 1.621 | 0.041 |
| 5 | 1.783 | 0.045 |
| 10 | 1.858 | 0.068 |
| 20 | 1.958 | 0.105 |

## Appendix

Table 2 shows the variation in full width at half maximum (FWHM) of the X-ray diffraction profiles obtained simultaneously with the residual stress, published in our previous report [14]. The table also shows the depth, $\zeta_F$, with CP processing time, $t_p$, which has the same FWHM as that at the surface of the NP specimen. The FWHM depends on the dislocations. From Table 2, the FWHM increases with $t_p$. However, $\zeta_F$ at $t_p \leq 5$ s/mm is lower than $d_1$ in Fig. 2(b). Especially, $\zeta_F$ for the CP specimen at $t_p \leq 1$ s/mm is much smaller than $d_1$. $\zeta_F$ at $t_p = 10$ and 20 s/mm affects the depth to $d_2$ in Fig. 2(b). In addition, the FWHM of the SP specimen at the surface is 2.020 deg, and $\zeta_F$ is 0.25 mm.

## References

1. Masaki, K., Ochi, Y., Ishii, A.: Fatigue properties of hard shot-peened SUS316L—behavior of hardness distribution, residual stress distribution and fatigue cracks during the fatigue process. Mater. Sci. Res. Int. **4**(3), 200–205 (1998)
2. Soyama, H.: Improvement of fatigue strength by using cavitating jets in air and water. J. Mater. Sci. **42**(16), 6638–6641 (2007)
3. Sano, Y., Obata, M., Kubo, T., Mukai, N., Yoda, M., Masaki, K., Ochi, Y.: Retardation of crack initiation and growth in austenitic stainless steels by laser peening without protective coating. Mater. Sci. Eng. A **417**(1–2), 334–340 (2006)
4. Soyama, H.: Introduction of compressive residual stress using a cavitating jet in air. Trans. ASME J. Eng. Mater. Technol. **126**(1), 123–128 (2004)
5. Blodgett, M.P., Nagy, P.B.: Eddy current assessment of near-surface residual stress in shot-peened nickel-base superalloys. J. Nondestruct. Eval. **23**(3), 107–123 (2004)
6. Zhou, J., Chen, K., Dover, W.D.: Uniform ac field in anisotropic bar and alternating current potential difference stress measurement. J. Phys. D, Appl. Phys. **32**(14), 1600–1604 (1999)
7. Blaow, M., Evans, J.T., Shaw, B.A.: The effect of microstructure and applied stress on magnetic Barkhausen emission in induction hardened steel. J. Mater. Sci. **42**(12), 4364–4371 (2007)
8. Shen, Y., Lee, C., Lo, C.C.H., Nakagawa, N., Frishman, A.M.: Conductivity profile determination by eddy current for shot-peened superalloy surfaces toward residual stress assessment. J. Appl. Phys. **101**(1), 014907 (2007)

9. Abu-Nabah, B.A., Nagy, P.B.: High-frequency eddy current conductivity spectroscopy for residual stress profiling in surface-treated nickel-base superalloys. NDT E Int. **40**(5), 405–418 (2007)
10. Sekine, Y., Soyama, H.: Evaluation of the surface of alloy tool steel treated by cavitation shotless peening using an eddy current method. Surf. Coat. Technol. **203**(16), 2254–2259 (2009)
11. Blaszkiewicz, M., Albertin, L., Junker, W.: The eddy current technique for determining residual stresses in steels. Mater. Sci. Forum **210–213**, 179–185 (1996)
12. Kittel, C.: Introduction to Solid State Physics, 8th edn. Wiley, New York (2005), pp. 133–159
13. Davis, J.R. (ed.): ASM Specialty Handbook: Stainless Steels. ASM International, Materials Park (1994),
14. Soyama, H., Kikuchi, T., Nishikawa, M., Takakuwa, O.: Introduction of compressive residual stress into stainless steel by employing a cavitating jet in air. Surf. Coat. Technol. **205**(10), 3167–3174 (2011)
15. Libby, H.L.: Introduction to Electromagnetic Nondestructive Test Methods. Wiley-Interscience, New York (1971), pp. 18–77
16. Cheng, C.C., Dodd, C.V., Deeds, W.E.: General analysis of probe coils near stratified conductors. Int. J. Nondestruct. Test., **3**(2), 109–130 (1971)
17. Li, Y., Theodoulidis, T., Tian, G.Y.: Magnetic field-based eddy-current modeling for multilayered specimens. IEEE Trans. Magn. **43**(11), 4010–4015 (2007)
18. Li, Y., Tian, G.Y., Simm, A.: Fast analytical modeling for pulsed eddy current evaluation. NDT E Int. **41**(6), 477–483 (2008)
19. Theodoulidis, T., Kriezis, E.: Series expansions in eddy current nondestructive evaluation models. J. Mater. Process. Technol. **161**(1–2), 343–347 (2005)
20. Bridgman, P.W.: The Physics of High Pressure. Dover, New York (1970), pp. 257–294